Pulse Index Modulation

Sultan Aldirmaz-Colak, *Senior Member, IEEE*, Erdogan Aydın, Yasin Celik, Yusuf Acar, and Ertugrul Basar, *Senior Member, IEEE*

***Abstract*— Emerging systems such as Internet-of-things (IoT) and machine-to-machine (M2M) communications have strict requirements on the power consumption of used equipments and associated complexity in the transceiver design. To meet these requirements, we propose a novel index modulation (IM) scheme, namely pulse index modulation (PIM) for single-input single-output (SISO) schemes. The proposed model uses well-localized and orthogonal Hermite-Gaussian pulses for data transmission and provides high spectral efficiency owing to the Hermite-Gaussian pulse indices. Considering the high complexity of maximum-likelihood (ML) detector, we propose a matched filtering-based low complexity detector to implement the PIM scheme in practice. Besides, it has been shown via analytical derivations and computer simulations that the proposed PIM system has better error performance and considerable signal-to-noise ratio (SNR) gain compared to existing spatial modulation (SM), code index modulation aided spread-spectrum (CIM-SS), CIM-SM, and traditional M-ary systems.**

***Index Terms*— Hermite-Gaussian pulses, Internet-of-Things (IoT), index modulation (IM), machine-to-machine (M2M), single-input single-output (SISO).**

I. Introduction

INTERNET-OF-THINGS (IoT) and machine-to-machine (M2M) communications are emerging technologies which are supported by 5th generation (5G) and and will likely be supported by 6th generation (6G). By 2025, it is expected that there will be more than 30 billion IoT connections, thus the efficient use of the spectrum comes to the fore in the system design [1]. IoT and M2M systems should have low-power equipments and low complexity. Therefore, single-input single-output (SISO) solutions are one step ahead of their multiple-input multiple-output (MIMO) counterparts.

MIMO transmission provides transmitter (Tx) and receiver (Rx) diversity gain and increases the data rate [2]. However, inter-antenna synchronization (IAS) and inter-antenna interference (IAI) are big problems of MIMO schemes. In 2008, Mesleh *et al.* proposed a novel transmission scheme, namely spatial modulation (SM) to overcome the aforementioned problems of MIMO systems [3]. SM has attracted quite a lot of attention from researchers [4]–[6]. According to this technique, only one antenna is activated among all transmit antennas for transmission at one symbol duration. Thus, IAI and IAS requirement are avoided. However, it is stated in [4], [5] that antenna switching in each symbol duration results in decreasing spectral efficiency (SE) in practice. Moreover, only one RF chain is sufficient in the SM, still multiple antennas are needed. To further exploit indexing mechanisms, the concept of SM has been generalized to other resources of communication systems and index modulation (IM) has emerged. For instance, Basar *et al.* proposed orthogonal frequency division multiplexing index modulation (OFDM-IM) that provides not only higher SE but also improved performance compared to classical OFDM [7]. To further improve SE compared to OFDM-IM, Mao *et al.* proposed dual-mode OFDM-IM [8] which utilizes entire subcarriers for symbol transmission, unlike OFDM-IM. These techniques become very popular, then their variants have been proposed in a very short time [9]–[11]. Moreover, in the recent past, IM has been utilized to select orthogonal codes in code-division multiple access (CDMA) communication [12], [13]. Both OFDM and CDMA are utilized for wideband communication however, their complexities are relatively high. Recently, a novel filter shape IM (FSIM) scheme has been proposed in [14]. In this letter, different filter shapes are obtained by optimization under a few constraints to provide minimum correlation among them. To avoid inter-symbol interference (ISI), FSIM requires ISI cancelation block in the receiver, which leads to an increase in the computational complexity.

Hermite-Gaussian pulses are widely used in ultra wideband communication [15], [16]. In [15], the authors proposed a spectrum efficient communication system that uses a summation of binary phase shift-keying (BPSK) modulated Hermite-Gaussian pulses with different orders. Since these pulses are orthogonal to each other, the transmission of a linear combination of these pulses that carries different symbols provides higher SE.

In this letter, we propose a novel IM scheme that activates certain Hermite-Gaussian pulse shape(s) for transmission instead of antenna indices according to the incoming information bits. Unlike SM and OFDM-IM systems, to generate the transmitted signal, the proposed pulse index modulation (PIM) does not require any transceiver components such as antennas or any complex operations such as FFT/IFFT. Thus, the transmitter of PIM has relatively low complexity, it is suitable for M2M or IoT applications.

Manuscript received March 26, 2021; revised April 7, 2021; accepted April 13, 2021. Date of publication April 16, 2021; date of current version July 10, 2021. The work of Ertugrul Basar was supported by TUBITAK under Grant 218E035. The associate editor coordinating the review of this letter and approving it for publication was M. Wen. *(Corresponding author: Sultan Aldirmaz-Colak.)*

Sultan Aldirmaz-Colak is with the Department of Electronics and Communication Engineering, Kocaeli University, 41380 İzmit, Turkey (e-mail: sultan.aldirmaz@kocaeli.edu.tr).

Erdogan Aydın is with the Department of Electrical and Electronics Engineering, Istanbul Medeniyet University, 34857 Istanbul, Turkey (e-mail: erdogan.aydin@medeniyet.edu.tr).

Yasin Celik is with the Department of Electrical and Electronics Engineering, Aksaray University, 68100 Aksaray, Turkey (e-mail: yasincelik@aksaray.edu.tr).

Yusuf Acar is with the Group of Electronic Warfare Systems, STM Defense Technologies Engineering Inc., 06510 Ankara, Turkey (e-mail: yusuf.acar@stm.com.tr).

Ertugrul Basar is with the CoreLab, Department of Electrical and Electronics Engineering, Koç University, 34450 Istanbul, Turkey (e-mail: ebasar@ku.edu.tr).

Digital Object Identifier 10.1109/LCOMM.2021.3073753

Since consecutive symbols are overlapped in the FSIM scheme, ISI occurs. However, in our system model, consecutive symbols do not overlap and ISI does not occur. Moreover, owing to the orthogonality among the Hermite-Gaussian pulses, more than one symbol can be sent in the same symbol duration.

The main contributions of the letter are summarized as follows:

- We introduce a novel PIM scheme for SISO systems. Similar to SM, index bits are used as an extra dimension to convey data bits besides conventional constellation mapping.
- We propose two receiver models: matched filtering-based low complexity detector and maximum likelihood (ML) detector.
- We propose the transmission of more than one pulse to increase the SE of the PIM technique, more than one pulse ($k \geq 2$) can be sent together owing to orthogonality property of Hermite-Gaussian pulses.
- We also obtain the average bit error probability (ABEP) for the ML detector. ABEP results match well with the simulation results.

The remainder of this letter is organized as follows. In Section II, we introduce the system model of PIM. In Section III, performance analysis of the proposed scheme is presented. Simulation results and performance comparisons are given in Section IV. Finally, the letter is concluded in Section V. [1]

II. System Model of Pulse Index Modulation

A. Hermite-Gaussian Pulse Family

We constitute a set of Hermite-Gaussian functions $\psi_v(t)$ that span the Hilbert space. These functions are known for their ability to be highly localized in time and frequency domains. They are defined by a Hermite polynomial modulated with a Gaussian function as

$$\psi_v(t) = \frac{2^{1/4}}{\sqrt{2^v v!}} H_v(\sqrt{2\pi}t) e^{-\pi t^2}, \tag{1}$$

where t represents time index, v is the order of Hermite-Gaussian function, and $H_v(t)$ is the Hermite polynomial series that is expressed as $H_v(t) = (-1)^v e^{t^2} \frac{\partial^v}{\partial t^v} e^{-t^2}$.

A number of Hermite polynomials can be given for $v = 0, 1, 2, 3$ as follows: $H_0(t) = 1$, $H_1(t) = 2t$, $H_2(t) = 4t^2 - 2$, $H_3(t) = 8t^3 - 12t$. One of the important properties of Hermite-Gaussian functions is orthogonality among them, which can be expressed as $\int_0^\infty \psi_m(t)\psi_n(t)dt = 0$ for $m \neq n$ [17]. Representation of Hermite-Gaussian pulses $\psi_0(t)$, $\psi_1(t)$, $\psi_2(t)$, and $\psi_3(t)$ in the time-domain are shown in Fig. 1(a) for $v = 0, 1, 2, 3$. As seen from Fig. 1(a), as the order of Hermite-Gaussian pulse increases, the oscillation of the pulse also increases. The frequency-domain representation

[1] ***Notation***: Throughout the letter, scalar values are italicized, vectors/matrices are presented by bold lower/upper case symbols. $*$ represents convolution operator. The transpose and the conjugate transpose are denoted by $(\cdot)^T$ and $(\cdot)^H$. $\lfloor . \rfloor$, $||.||$, and $C(.,.)$ represent the floor operation, Euclidean norm, and Binomial coefficient, respectively. $\mathcal{CN}(0, \sigma^2)$ represents the complex Gaussian distribution with zero mean and variance σ^2 and $\mathbf{I}_n$ is the $n \times n$ identity matrix. Last, $\frac{\partial}{\partial t}$ represents partial derivative.

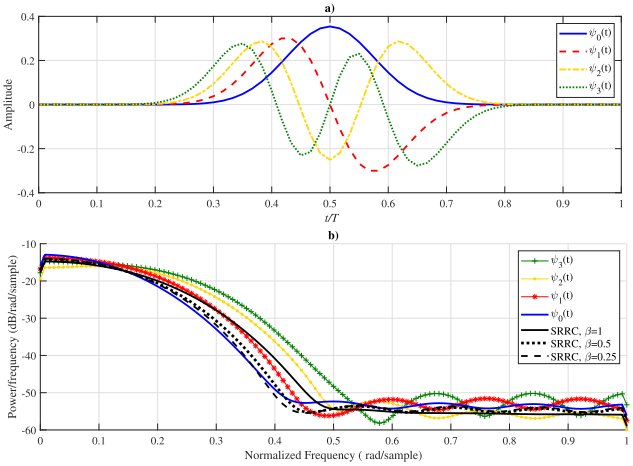

Fig. 1. Different Hermite-Gaussian pulses (a) with $L = 127$ in time-domain (b) bandwidth comparison with SRRC in frequency-domain.

of the these Hermite-Gaussian pulses and square root raised cosine (SRRC) pulse with different roll-off factors (β) are given in Fig. 1(b). We can state two important issues from Fig. 1(b). First, the bandwidth of the Hermite-Gaussian pulses increases with the increase of order, as the first-null bandwidth is considered. Second, the bandwidth of the zeroth and the first order Hermite-Gaussian pulses are narrower than that of SRRC, while the bandwidth of the second and the third order Hermite-Gaussian pulses are wider. In other words, as can be seen from Fig. 1(b), the bandwidth usage of the proposed scheme is relatively higher than the SRRC with $\beta = 1$.

B. PIM Transmission Model

The transceiver block diagram of the proposed PIM scheme is represented in Fig. 2. In the PIM scheme, firstly, incoming bit sequence $\mathbf{b} = [\mathbf{b}_1, \mathbf{b}_2]$ with the size of $\left(1 \times p_{\text{PIM}}\right)$ is splitted into pulse index selector and serial-to-paralel (S/P) converter blocks. S/P converter splits the $\mathbf{b}_2$ bit sequence with length of $p_2 = k \log 2(M)$ into k subblocks. The bit sequence $\mathbf{b}_{2,k}$ of each subblock is used as an input for M-ary signal constellation diagram block which outputs the modulated symbol. Then, the $\mathbf{b}_1$ bit sequence with length of $p_1 = \left\lfloor \log_2 \binom{n}{k} \right\rfloor$ determines indices of k active pulses where n is the total number of pulses in the set. k-th modulated symbol is multiplied with k-th selected pulse, $k \in \{1, \ldots k\}$. Last, outputs of multiplier blocks are summed. Then, the signal is sent to the RF chain.

The baseband PIM signal to be transmitted for k can be expressed as

$$x(t) = \frac{1}{\sqrt{k}} \sum_{m=-\infty}^{\infty} \sum_{j=1}^{k} s_{i,j} \psi_{\ell_j}(t - mT_{sym}), \tag{2}$$

where $s_{i,j}$ represents the i-th M-ary symbol corresponding to $\mathbf{b}_{2,k}$, i.e., $s_{i,j} \in \{s_1, s_2, \ldots s_M\}$, which is carried on $\psi_{\ell_j}(t)$. $\psi_{\ell_j}(t)$ is the j-th element in row ℓ of the look-up table, where $j \in \{1, 2, \ldots 2^{p_1}\}$, and T_{sym} denotes the pulse duration. $\frac{1}{\sqrt{k}}$ is a normalization coefficient used to make the total symbol energy $E_s = 1$. For example, analytical expressions of the possible transmitted symbols for $k = 1$ with BPSK modulation (i.e. $s_{i,j} = \pm 1$) in the time-domain are given in Table I.

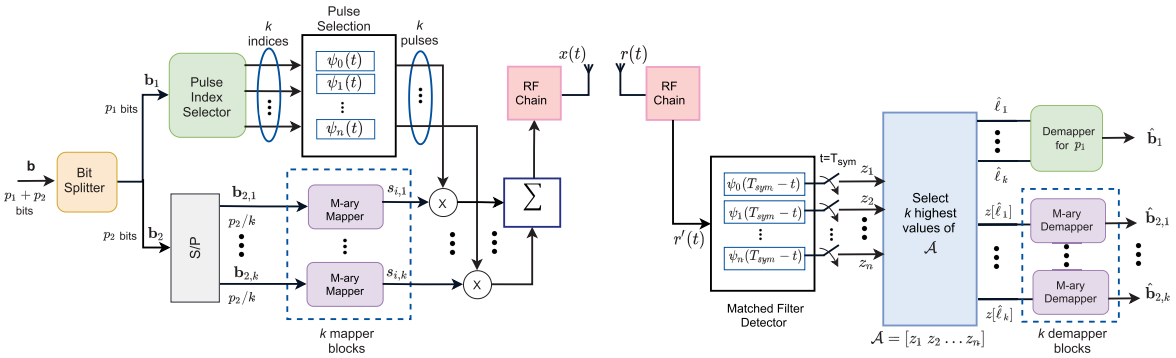

Fig. 2. The transceiver block diagram of the PIM scheme.

TABLE I

POSSIBLE PULSES AND THEIR ANALYTICAL EXPRESSIONS FOR $n = 4$, $k = 1$, AND $p_1 = 2$

Possible Pulses for BPSK	Analytical Expressions
$\pm\psi_0(t)$	$\pm 2^{1/4} e^{-\pi t^2}$
$\pm\psi_1(t)$	$\pm 2^{1/4}(2\sqrt{\pi}) t e^{-\pi t^2}$
$\pm\psi_2(t)$	$\pm \frac{2^{1/4}}{2\sqrt{2}}(8\pi t^2 - 2) e^{-\pi t^2}$
$\pm\psi_3(t)$	$\pm 2^{1/4} \left(\frac{4\pi\sqrt{2\pi} t^3 - 3\sqrt{2\pi} t}{\sqrt{3}} \right) e^{-\pi t^2}$

TABLE II

A REFERENCE LOOK-UP TABLE FOR $n = 4$, $k \in \{1, 2\}$, AND $p_1 = 2$

Index Bits	Selected Pulse for PIM scheme ($k = 1$)	Selected Pulse for PIM scheme ($k = 2$)
$\{0, 0\}$	$\{\ \psi_0(t)\}$	$\{\psi_0(t),\ \psi_1(t)\ \}$
$\{0, 1\}$	$\{\ \psi_1(t)\}$	$\{\psi_0(t),\ \psi_2(t)\ \}$
$\{1, 0\}$	$\{\ \psi_2(t)\}$	$\{\psi_1(t),\ \psi_2(t)\ \}$
$\{1, 1\}$	$\{\ \psi_3(t)\}$	$\{\psi_1(t),\ \psi_3(t)\ \}$

The number of transmitted bits per channel use (bpcu) of the PIM scheme can be calculated as $p_{\text{PIM}} = p_1 + p_2$ bpcu. While the classical SISO system with $M = 2$ obtains 1 bpcu at each symbol duration, PIM scheme transmits $p_{\text{PIM}} = 3$ bits and 4 bits for $k = 1$ and $k = 2$, respectively.

A look-up table, which maps the index bits to transmitted pulses for $k = \{1, 2\}$ and $n = 4$, is given in Table II. If the information bit block is given as $\mathbf{b} = [0\ 0\ 1\ 0]$ for $k = 2$, the selected Hermite-Gaussian pulses are zeroth order and the first order ones according to the first two bits (the first row ($\ell = 1$) of the look-up table), and selected BPSK symbols are $s_{i,1} = 1$ and $s_{i,2} = -1$. Thus, the transmitted signal can be expressed as $x(t) = \frac{1}{\sqrt{2}}\big(\boldsymbol{\psi}_0(t) - \boldsymbol{\psi}_1(t)\big)$, if BPSK modulation is applied. As Hermite-Gaussian pulses are orthogonal to each other, the modulation type can be thought as quadrature phase shift-keying (QPSK). We propose two different receiver model to detection of PIM scheme.

1) Matched Filter Detection of PIM Scheme: The noisy received signal in time-domain can be represented as

$$r(t) = h(t) * x(t) + w(t), \tag{3}$$

where $h(t)$ and $w(t)$ represent impulse response of the flat-fading channel and additive white Gaussian noise (AWGN), respectively. Since Hermite-Gaussian functions and their linear combinations are orthogonal to each other, only n times ($n \leq 2^{p_1}$) matched filtering computation is enough to estimate $\hat{\mathbf{b}}_1$. This reduces the computational complexity since n is less than the number of rows of the look-up table, i.e., 2^{p_1} for $k \geq 3$.

In Fig. 2, after the RF chain module, the signal $r'(t)$ is sent to n-branch matched filtering blocks. The outputs of the mached filters are sampled at each T_{sym} instant and $\mathbf{z} = [z_1, z_2, \dots z_n]$ is obtained as follows:

$$z_v = < r'(t), \psi_v(t) > = \int_0^{T_{sym}} r'(t)\psi_v(t)\mathrm{d}t, \quad v = 1, 2, \dots n. \tag{4}$$

After elements of $\mathbf{z}$ are ordered according to their magnitudes, i.e., $\mathcal{A} = |\mathbf{z}|$ and the highest k out of n values in $\mathcal{A}$ are selected with their indices and complex values. Hence, the transmitted pulse indices $(\hat{\ell}_1, \hat{\ell}_2, \dots, \hat{\ell}_k)$ have been obtained. While the estimates of index information are sent to the demapper for the estimation of $\hat{\mathbf{b}}_1$, the corresponding k complex-samples, i.e., $[z(\hat{\ell}_1), z(\hat{\ell}_2), \dots z(\hat{\ell}_k)]$ are sent to M-ary demapper blocks. Thus, $\hat{\mathbf{b}}_2 = [\hat{\mathbf{b}}_{2,1}\hat{\mathbf{b}}_{2,2}, \dots \hat{\mathbf{b}}_{2,k}]$ is estimated. The computational complexity of this detector is $\mathcal{O}_{MF}(n \times L)$.

2) ML Detection of PIM Scheme: After the perfect carrier detection and sampling at the output of the channel, the vector representation of the received baseband signal for PIM scheme can be expressed as follows:

$$\begin{aligned} \mathbf{r}_{\text{PIM}} &= \mathbf{x}h + \mathbf{w} \\ &= \left(\frac{1}{\sqrt{k}} \sum_{j=1}^{k} s_{i,j} \boldsymbol{\psi}_{\ell_j} \right) h + \mathbf{w}, \end{aligned} \tag{5}$$

where $\mathbf{w} \in \mathcal{C}^{L \times 1}$ is the noise vector with elements following $\mathcal{CN}(0, \frac{N_0}{2}\mathbf{I}_L)$, h represents the complex Rayleigh fading coefficient. $\boldsymbol{\psi}_{\ell_j}$ is the discrete representation of the Hermite-Gaussian pulses obtained from the continuous Hermite-Gaussian pulses by using the Nyquist sampling theorem ($\psi_{\ell_j}(t) = \psi_{\ell_j}[lT_s]$, where l is an integer ($l = 0, 1, \dots L$, here L is the number of samples of the j^{th} Hermite-Gaussian pulse) and T_s denotes the sampling interval).

ML detector for PIM scheme can be given as follows:

$$\begin{aligned} &\left(\hat{s}_{i,1}, \dots, \hat{s}_{i,k}, \hat{\ell}_1, \dots, \hat{\ell}_k\right) = \\ &= \underset{\substack{s_{i,1},\dots,s_{i,k} \\ \ell_1,\dots,\ell_k}}{\arg\max} \left(\Pr\left(\mathbf{r}_{\text{PIM}} | s_{i,1}, \dots, s_{i,k}, \boldsymbol{\psi}_{\ell_1}, \dots, \boldsymbol{\psi}_{\ell_k} \right) \right) \\ &= \underset{\substack{s_{i,1},\dots,s_{i,k} \\ \ell_1,\dots,\ell_k}}{\arg\min} \left\{ \left\| \mathbf{r}_{\text{PIM}} - \left(\frac{1}{\sqrt{k}} \sum_{j=1}^{k} s_{i,j} \boldsymbol{\psi}_{\ell_j} \right) h \right\|^2 \right\}. \end{aligned} \tag{6}$$

For simplicity, the ML detectors for PIM scheme only for $k = 1$ and $k = 2$ can be expressed respectively as

$\left(\hat{s}_i, \hat{\ell}\right) = \underset{s_i,\ell}{\arg\min}\left\{\left|\left|\mathbf{r}_{\text{PIM}} - h s_i \boldsymbol{\psi}_\ell\right|\right|^2\right\}$ and $\left(\hat{s}_{i,1}, \hat{s}_{i,2}, \hat{\ell}_1, \hat{\ell}_2\right) = \underset{s_{i,1}, s_{i,2}, \ell_1, \ell_2}{\arg\min}\left\{\left|\left|\mathbf{r}_{\text{PIM}} - \frac{1}{\sqrt{2}}\left(s_{i,1}\boldsymbol{\psi}_{\ell_1} + s_{i,2}\boldsymbol{\psi}_{\ell_2}\right)h\right|\right|^2\right\}$.

Finally, using the detected $(\hat{s}_{i,1}, \ldots, \hat{s}_{i,k}, \hat{\ell}_1, \ldots, \hat{\ell}_k)$ values, the originally transmitted bit sequence $\hat{\mathbf{b}}$ is reconstructed at the receiver with the help of the index to bits mapping technique as shown at the receiver block of the PIM system. The computational complexity of this detector is $\mathcal{O}_{ML}(2^{p_1+p_2} \times L)$.

III. Performance Analysis

In this section, we analyze the ABEP performance of the PIM scheme. Accordingly, using the well-known union bounding technique as in [18], the expression of ABEP $\mathbb{P}$ for proposed scheme can be given as follows:

$$\mathbb{P} \leq \frac{1}{2^{p_{\text{PIM}}}} \sum_{d=1}^{2^{p_{\text{PIM}}}} \sum_{u=1}^{2^{p_{\text{PIM}}}} \frac{\mathbb{P}_{\text{e}}\left(\boldsymbol{\xi}_d \to \hat{\boldsymbol{\xi}}_u\right) N(d,u)}{p_{\text{PIM}}}, \tag{7}$$

where $p_{\text{PIM}} = p_1 + p_2$ is the number of bits transmitted in active pulse indices and modulated symbols, $N(d,u)$ is expressed as the number of bits in errors between the vectors $\boldsymbol{\xi}_d$ and $\hat{\boldsymbol{\xi}}_u$. $\mathbb{P}_{\text{e}}\left(\boldsymbol{\xi}_d \to \hat{\boldsymbol{\xi}}_u\right)$ is the APEP of deciding $\hat{\boldsymbol{\xi}}_u$ giving that $\boldsymbol{\xi}_d$ is transmitted and it can be expressed as

$$\mathbb{P}_{\text{e}}\left(\boldsymbol{\xi}_d \to \hat{\boldsymbol{\xi}}_u\right) = \frac{1}{2}\left(1 - \sqrt{\frac{\sigma_{k,\alpha}^2}{1+\sigma_{k,\alpha}^2}}\right), \tag{8}$$

where, $\sigma_{k,\alpha}^2$ can be given for $k = 1$ and $k = 2$ given respectively as follows:

$$\sigma_{1,\alpha}^2 = \begin{cases} \frac{E_s}{2N_0}\sigma_h^2\left(|s_i|^2 + |\hat{s}_i|^2\right) \text{ if } \boldsymbol{\psi}_j \neq \boldsymbol{\psi}_{\hat{j}} \\ \frac{E_s}{2N_0}\sigma_h^2\left(|s_i - \hat{s}_i|^2\right) \text{ if } \boldsymbol{\psi}_j = \boldsymbol{\psi}_{\hat{j}} \end{cases} \tag{9}$$

$$\sigma_{2,\alpha}^2 = \begin{cases} \frac{E_s}{2N_0}\sigma_h^2\left(|s_{i,1}|^2 + |\hat{s}_{i,1}|^2 + |s_{i,2}|^2 + |\hat{s}_{i,2}|^2\right) \\ \quad \text{if } \boldsymbol{\psi}_{\ell_1} \neq \boldsymbol{\psi}_{\hat{\ell}_1}, \boldsymbol{\psi}_{\ell_2} \neq \boldsymbol{\psi}_{\hat{\ell}_2} \\ \frac{E_s}{2N_0}\sigma_h^2\left(|s_{i,1} - \hat{s}_{i,1}|^2 + |s_{i,2}|^2 + |\hat{s}_{i,2}|^2\right) \\ \quad \text{if } \boldsymbol{\psi}_{\ell_1} = \boldsymbol{\psi}_{\hat{\ell}_1}, \boldsymbol{\psi}_{\ell_2} \neq \boldsymbol{\psi}_{\hat{\ell}_2} \\ \frac{E_s}{2N_0}\sigma_h^2\left(|s_{i,1}|^2 + |\hat{s}_{i,1}|^2 + |s_{i,2} - \hat{s}_{i,2}|^2\right) \\ \quad \text{if } \boldsymbol{\psi}_{\ell_1} \neq \boldsymbol{\psi}_{\hat{\ell}_1}, \boldsymbol{\psi}_{\ell_2} = \boldsymbol{\psi}_{\hat{\ell}_2} \\ \frac{E_s}{2N_0}\sigma_h^2\left(|s_{i,1} - \hat{s}_{i,1}| + |s_{i,2} - \hat{s}_{i,2}|^2\right) \\ \quad \text{if } \boldsymbol{\psi}_{\ell_1} = \boldsymbol{\psi}_{\hat{\ell}_1}, \boldsymbol{\psi}_{\ell_2} = \boldsymbol{\psi}_{\hat{\ell}_2} \end{cases} \tag{10}$$

where σ_h^2 is the variance of Rayleigh fading channel coefficient and $\sigma_h^2 = 1$. Consequently, by substituting (9) and (8) into (7), we obtain the ABEP for PIM system for ML detector, and similarly, by substituting (10) and (8) into (7), we obtain the ABEP for $k > 2$ system.

IV. Simulation Results

To demonstrate the improved performance of the proposed techniques, the bit error rate (BER) of PIM systems is evaluated with different system setups. Generalized code index modulation aided SM (GCIM-SM) [13], CIM-spread spectrum (CIM-SS) [12], SM, traditional M-PSK/QAM schemes are selected as benchmarks. The SNR used in computer simulations herein is defined as E_s/N_0 where E_s is energy per symbol and N_0 is the noise power. Each Hermite-Gaussian pulse consists of 127 samples. Since the head and tail of the blows contain a large number of zero-value samples, we truncate their edges and downsample each pulse with 3. Thus, each pulse includes 16 samples. Since the order of Hermite-Gaussian pulses increases, the time signal oscillation also increases. Therefore, the pulses include fewer zeros at the head and the tail. The considered interval can be determined by using 98% energy criteria. All simulations are performed over frequency-flat Rayleigh fading channels. We assume that the channel is constant during one symbol duration, and the channel state information (CSI) is perfectly known at the receiver.

The theoretical (with ML) and simulations (ML&MF) average BER performance curves of the PIM scheme with M-PSK, $M = 4, 8, 16, 32$, $n = 4$, and $k = 1$ are presented for $p_{\text{PIM}} = 4, 5, 6$, and 7 bits in Fig. 3 (a). Here, the PIM technique transmits $4, 5, 6$, and 7 bits by 2 bits with active pulse indices and $2, 3, 4$, and 5 bits with the transmitted symbols, respectively. As can be seen from Fig. 3 (a), analytical results for ML receiver match simulation results well particularly at high modulation order. Owing to orthogonality among Hermite-Gaussian pulses, MF detector performance almost equal to ML detector.

In Fig. 3(b), to investigate the effect of k on the PIM performance, which is set to $\{1, 2, 3\}$ and BER performance is obtained. For $k = 1$ and $k = 3$, one pulse and three pulses are selected for transmission simultaneously, where one QPSK or three QPSK symbols are conveyed, respectively. By selecting three pulse shapes out of the set instead of one pulse shape, extra five bits can be transmitted when the QPSK scheme is employed for each pulse. In this case, as seen from Fig. 3(b) almost 5 dB SNR is required to reach the same BER value. As k increases, n and look-up table complexity increase as well. For example for $k = 3$, the pulse set cardinality should be $n = 5$. Also, BER performance curves of GCIM-SM with $n_T = 8, p_c = 2, M = 4$-QAM and CIM-SS $n_T = 1, p_c = 2, M = 32$-QAM systems, where n_T and p_c denote the numbers of transmit antennas and conveyed bits in the code index, are compared with the proposed PIM scheme. As seen from Fig. 3(b), PIM scheme has better BER performance compared to GCIM-SM and CIM-SS schemes for 9 bpcu.

The average BER performance curves of the PIM, and benchmarks schemes are shown in Fig. 3(c) for M-PSK/QAM at 6 bpcu. PIM technique carries 2 bits with active pulse indices and 4 bits with the transmitted symbol; In the SM technique, 2 bits are transmitted in antenna indices and 4 bits are transmitted with symbols. As seen from Fig. 3(c), the PIM scheme ($k = 2$) provides better performance with approximately 1 dB SNR gain compared to PIM system when QAM is used. Also, the analytical and the simulation results match well. The proposed PIM scheme has also better BER performance compared to SM and traditional QAM schemes.

Fig. 4 presents average BER performance curves of PIM, SM, and traditional QAM schemes for (a) 8 bpcu and (b) 10 bpcu. For Fig. 4(a), PIM ($k = 2$) carries 2 bits with active pulse indices and 6 bits with the transmitted symbol; the SM scheme carries 3 bits with antenna indices and 5 bits with the transmitted symbol. The corresponding values in Fig. 4(b) are 2 and 8 bits for PIM; 3 and 7 bits for SM schemes, respectively. We can see from Fig. 4 that PIM scheme has a considerable SNR gain compared to SM scheme for the same

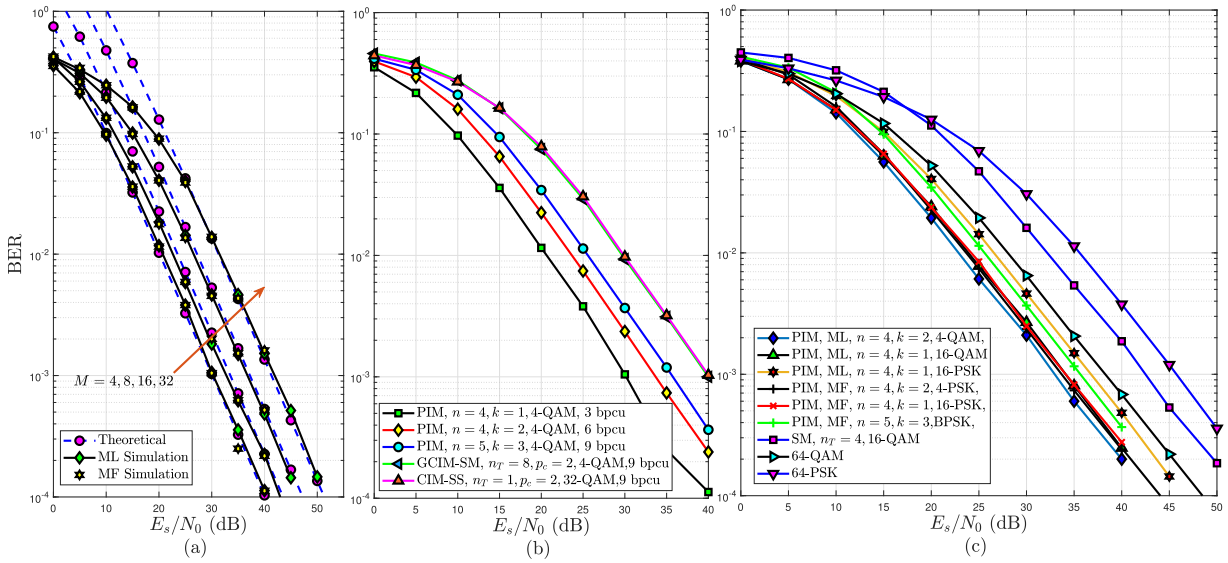

Fig. 3. E_s/N_0 vs. BER values of PIM and various benchmark schemes with various parameters.

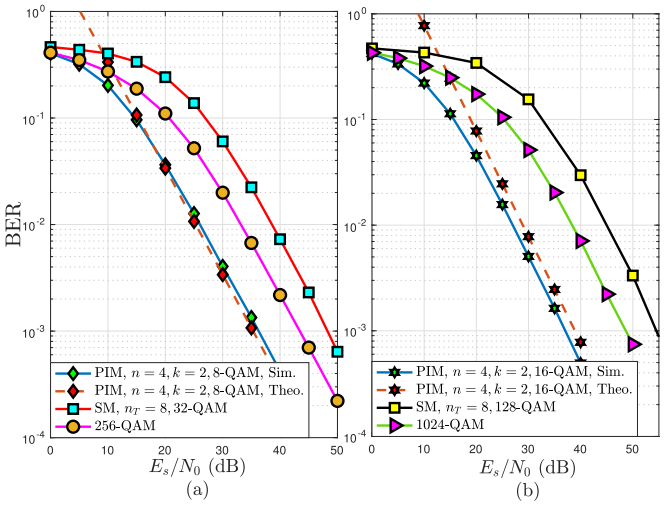

Fig. 4. Performance comparisons of SM, and traditional QAM systems for (a) 8 bpcu (b) 10 bpcu.

bpcu. At BER $= 10^{-2}$, the proposed scheme requires almost 18 dB less power compared to SM scheme for $M = 16$ case.

V. Conclusion

We have proposed a new IM scheme, namely PIM, which exploits the indices of Hermite-Gaussian pulses for SISO systems. A low complexity detector based on matched filter is also proposed. Its performance is presented in comparison with ML detector. Analytical expressions for average BER of the PIM for $k = \{1, 2\}$ system has been derived and its superiority has been shown. This method is suitable for systems that need low complexity owing to their SISO structure. For this reason, we think that our scheme can be utilized especially in M2M and IoT applications and it can be generalized to different orthogonal pulses.

References

[1] S. Dang, O. Amin, B. Shihada, and M.-S. Alouini, "What should 6G be?" *Nature Electron.*, vol. 3, no. 1, pp. 20–29, Jan. 2020.

[2] E. Telatar, "Capacity of multi-antenna Gaussian channels," *Eur. Trans. Telecommun.*, vol. 10, no. 6, pp. 585–595, Nov. 1999.

[3] R. Y. Mesleh, H. Haas, S. Sinanovic, C. W. Ahn, and S. Yun, "Spatial modulation," *IEEE Trans. Veh. Technol.*, vol. 57, no. 4, pp. 2228–2241, Jul. 2008.

[4] C. A. F. D. Rocha, B. F. Uchoa-Filho, and D. Le Ruyet, "Study of the impact of pulse shaping on the performance of spatial modulation," in *Proc. Int. Symp. Wireless Commun. Syst. (ISWCS)*, Aug. 2017, pp. 303–307.

[5] K. Ishibashi and S. Sugiura, "Effects of antenna switching on band-limited spatial modulation," *IEEE Wireless Commun. Lett.*, vol. 3, no. 4, pp. 345–348, Aug. 2014.

[6] M. Wen *et al.*, "A survey on spatial modulation in emerging wireless systems: Research progresses and applications," *IEEE J. Sel. Areas Commun.*, vol. 37, no. 9, pp. 1949–1972, Sep. 2019.

[7] E. Başar, U. Aygölü, E. Panayırcı, and H. V. Poor, "Orthogonal frequency division multiplexing with index modulation," *IEEE Trans. Signal Process.*, vol. 61, no. 22, pp. 5536–5549, Nov. 2013.

[8] T. Mao, Z. Wang, Q. Wang, S. Chen, and L. Hanzo, "Dual-mode index modulation aided OFDM," *IEEE Access*, vol. 5, pp. 50–60, 2017.

[9] C.-C. Cheng, H. Sari, S. Sezginer, and Y. T. Su, "Enhanced spatial modulation with multiple signal constellations," *IEEE Trans. Commun.*, vol. 63, no. 6, pp. 2237–2248, Jun. 2015.

[10] S. A. Çolak, Y. Acar, and E. Basar, "Adaptive dual-mode OFDM with index modulation," *Phys. Commun.*, vol. 30, pp. 15–25, Oct. 2018.

[11] J. Li, S. Dang, M. Wen, X.-Q. Jiang, Y. Peng, and H. Hai, "Layered orthogonal frequency division multiplexing with index modulation," *IEEE Syst. J.*, vol. 13, no. 4, pp. 3793–3802, Dec. 2019.

[12] G. Kaddoum, M. F. A. Ahmed, and Y. Nijsure, "Code index modulation: A high data rate and energy efficient communication system," *IEEE Commun. Lett.*, vol. 19, no. 2, pp. 175–178, Feb. 2015.

[13] F. Cogen, E. Aydin, N. Kabaoglu, E. Basar, and H. Ilhan, "Generalized code index modulation and spatial modulation for high rate and energy-efficient MIMO systems on Rayleigh block-fading channel," *IEEE Syst. J.*, vol. 15, no. 1, pp. 538–545, Mar. 2021.

[14] M. Saad, J. Palicot, F. Bader, A. C. A. Ghouwayel, and H. Hijazi, "A novel index modulation dimension based on filter domain: Filter shapes index modulation," *IEEE Trans. Commun.*, vol. 69, no. 3, pp. 1445–1461, Mar. 2021.

[15] S. Aldirmaz, A. Serbes, and L. Durak-Ata, "Spectrally efficient OFDMA lattice structure via toroidal waveforms on the time-frequency plane," *EURASIP J. Adv. Signal Process.*, vol. 2010, no. 1, Dec. 2010, Art. no. 684097.

[16] T. Kurt, G. K. Kurt, and A. Yongacoglu, "Throughput enhancement in multi-carrier systems employing overlapping weyl-heisenberg frames," in *Proc. IEEE Int. Conf. Commun.*, Jun. 2009, pp. 1–6.

[17] H. M. Ozaktas, Z. Zalevsky, and M. A. Kutay, *The Fractional Fourier Transform With Applications in Optics and Signal Processing*. New York, NY, USA: Wiley, 2001.

[18] J. G. Proakis, *Digital Communication*, 5th ed. New York, NY, USA: McGraw-Hill, 2008.